JOURNAL OF MATERIALS SCIENCE **36** (2001) 1671–1679

Effect of Er_2O_3 addition on the microstructure, electrical properties, and stability of Pr_6O_{11}-based ZnO ceramic varistors

CHOON-WOO NAHM, CHOON-HYUN PARK
Department of Electrical Engineering, Dongeui University, Pusan 614-714, Korea
E-mail: cwnahm@dongeui.ac.kr

The microstructure, electrical properties, and stability of Pr_6O_{11}-based ZnO varistors, which are composed of ZnO-Pr_6O_{11}-CoO-Er_2O_3 systems, were investigated with Er_2O_3 additive content. The density of ceramics was in the range of 84–88% of TD at 1300 °C and 93–98% of TD at 1350 °C, and greatly affected the stability. Most of the added-Er_2O_3 were segregated at nodal points. The varistors with 0.5 mol% Er_2O_3 sintered at 1300 °C exhibited the best nonlinear current-voltage characteristics, which the nonlinear exponent is 52.8 and the leakage current is 9.8 μA. All the varistors sintered at 1300 °C, even under relatively weak stress, exhibited the thermal runaway within short time in order of high leakage current. On the contrary, the stability of varistors sintered at 1350 °C exhibited far higher stability than that at 1300 °C. Particularly, the varistors with 0.5 mol% Er_2O_3 exhibited not only relatively good nonlinear current-voltage characteristics, which the nonlinear exponent is 34.8 and the leakage current is 7.4 μA, but also excellent stability, which the variation rates of varistor voltage, nonlinear exponent, and leakage current are below 1%, 3%, and 3%, respectively, even under more severe stress such as (0.80 $V_{1\,mA}$/90 °C/12 h) + (0.85 $V_{1\,mA}$/115 °C/12 h) + (0.90 $V_{1\,mA}$ /120 °C/12 h).

1. Introduction

ZnO varistors (variable resistors) are ceramic semiconductor devices formed by a ceramic sintering process, based to ZnO with a number of other metal oxides of small amount, in addition to varistor-forming oxides, such as Bi_2O_3 and Pr_6O_{11}. The current-voltage (I-V) characteristics of ZnO varistors is described by relation $I = K \cdot V^{\alpha}$, where α is the nonlinear exponent, which characterizes the nonlinear properties of varistors. Because of their high nonlinearity, high excellent surge withstanding capability, and fast response against transient abnormal voltage, ZnO varistors have been extensively used as the surge absorbers in electronic equipments and the core element of surge arresters in electric power systems, such as distribution and transmission lines [1, 2].

ZnO varistors are largely classified into two categories, called Bi_2O_3-based and Pr_6O_{11}-based varistors, in terms of varistor-forming oxides inducing the nonlinear properties of varistors [3]. Most of commercial ZnO varistors are Bi_2O_3-based varistors showing excellent varistor properties, but they have a few flaws due to Bi_2O_3 having a high volatility and reactivity [4]. The former changes varistor characteristics with the variation of inter-composition ratio of additives, the later destroys the multilayer structure of chip varistors, and it generates an additional insulating spinel phase, which does not play any role in electrical conduction. And another flaw of Bi_2O_3-based varistors needs many additives to obtain high nonlinearity and stable electrical properties.

Recently, Pr_6O_{11}-based varistors have been studied basically to solve problems related with Bi_2O_3 [5–7]. These varistors were reported to exhibit relatively high nonlinear exponent of 25–37 for only ternary system ZnO-Pr_6O_{11}-CoO, compared to Bi_2O_3-based ZnO varistors having nonlinear exponent of 13–18 for only ternary system ZnO-Bi_2O_3-CoO (or MnO). And they were reported to contain only two phases, namely, ZnO grains and intergranular layers, unlikely Bi_2O_3-based ZnO varistors having a spinel phase. The absence of spinel phase, which does not plays any electrical role at grain boundaries, increases an active grain boundary area through which the electric current flows. Therefore, the effective cross-section area of varistor element is increased. This gives rise to compacting of systems, variety in application field, and high performance as a surge protector. Really, the history of Pr_6O_{11}-based ZnO varistors is similar to that of Bi_2O_3-based ZnO varistors, but has not been actively studied. It is believed that the reason is, presumely, because of the expensive Pr_6O_{11}, the high sintering temperature, compared with Bi_2O_3-based varistors, and the good nonlinearity of Bi_2O_3-based varistors.

To apply Pr_6O_{11}-based varistors in various areas, the effect of the variables, such as the kind and amount of additives, composition ratio, sintering temperature, and cooling rate on the electrical properties, and stability

of Pr_6O_{11}-based varistors should be continuously studied. Most of the studies on Pr_6O_{11}-based varistors, up to now, have been limited to the ternary system ZnO-Pr_6O_{11}-CoO and further, no their stability has been reported. In quite recent, Nahm *et al*. reported Pr_6O_{11}-based varistors of 4- or 5-component systems having relatively good nonlinearity and particularly, very high stability [8–10]. Pr_6O_{11}-based ZnO varistors containing Er_2O_3 have not been yet studied in detail.

The purpose of this paper is to investigate the microstructure, current-voltage (I-V) characteristics, capacitance-voltage (C-V) chracteristics, and stability of ZPCE (ZnO-Pr_6O_{11}-CoO-Er_2O_3 based) varistors with Er_2O_3 additive content and to discuss their possibility of application.

2. Experimental procedure

2.1. Sample preparation

Reagent-grade raw materials were prepared for ZPCE varistors with composition expression, such as $(98.5 - x)$ mol% ZnO + 0.5 mol% Pr_6O_{11} + 1.0 mol% CoO + x mol% Er_2O_3 ($x = 0.0, 0.5, 1.0, 2.0$). Raw materials were mixed by ball milling with zirconia balls and acetone in a polypropylene bottle for 24 h. The mixture was dried at 120 °C for 12 h and calcined in air at 750 °C for 2 h. The calcined mixture was pulverized using an agate mortar/pestle and after 2 wt% polyvinyl alcohol (PVA) binder addition, granulated by sieving 100-mesh screen to produce starting power. The power was uniaxially pressed into discs of 10 mm in diameter and 2 mm in thickness at a pressure of 80 MPa. The discs were placed in the starting power using an alumina crucible, sintered at 1300 °C and 1350 °C in air for 1 h, and furnace-cooled to room temperature. The heating and cooling rates were 4 °C/min. The sintered samples were lapped and polished to 1.0 mm thickness. The size of the final samples was about 8 mm in diameter and 1.0 mm in thickness. The silver paste was coated on both faces of samples and the silver electrodes were formed by heating at 600 °C for 10 min. The size of electrodes was 5 mm in diameter.

2.2. I-V characteristics measurement

The current-voltage (I-V) characteristics of ZPCE varistors were measured using an I-V source/measure unit (Keithley 237). The varistor voltage ($V_{1\,mA}$) was measured at 1.0 mA/cm^2 and the leakage current (I_ℓ) was defined as the current at 0.80 $V_{1\,mA}$. In addition, the nonlinear exponent (α) is defined by $\alpha = 1/(\log E_2 - \log E_1)$, where E_2 and E_1 are the electric field corresponding to 10 mA/cm^2 and 1.0 mA/cm^2, respectively.

2.3. C-V characteristics measurement

The capacitance-voltage (C-V) characteristics of ZPCE varistors were measured at 1 kHz using a RLC meter (QuadTech 7600) and an electrometer (Keithley 670). The donor concentration (N_d) and the barrier height (ϕ_b) were determined by the equation $(1/C_b - 1/C_{bo})^2 = 2(\phi_b + V_{gb})/q\varepsilon N_d$ [12], where C_b is the capacitance per unit area of a grain boundary, C_{bo} is the value of C_b when $V_{gb} = 0$, V_{gb} is the applied voltage per grain boundary, q is the electronic charge, ε is the permittivity of ZnO ($\varepsilon = 8.5\varepsilon_o$). The density of interface states (N_t) at the grain boundary was determined by the equation $N_t = (2\varepsilon N_d \phi_b/q)^{1/2}$ [11] using the value of the donor concentration and barrier height obtained above. Once the donor concentration and barrier height are known, the depletion layer width (t) of the either side at the grain boundaries was determined by the equation $N_d t = N_t$ [12].

2.4. Stability tests

The stability tests were performed under the four continuous d.c. stress conditions, such as 0.80 $V_{1\,mA}$/90 °C/12 h in the first stress, (0.80 $V_{1\,mA}$/90 °C/12 h) + (0.85 $V_{1\,mA}$/115 °C/12 h) in the second stress, (0.80 $V_{1\,mA}$/90 °C/12 h) + (0.85 $V_{1\,mA}$/115 °C/12 h) + (0.90 $V_{1\,mA}$/120 °C/12 h) in the third stress, and (0.80 $V_{1\,mA}$/90 °C/12 h) + (0.85 $V_{1\,mA}$/115 °C/12 h) + (0.90 $V_{1\,mA}$/120 °C/12 h) + (0.95 $V_{1\,mA}$/150 °C/12 h) in the fourth stress. And at the same time, the leakage current during the stress time was monitored at intervals of 1 min by an I-V source/measure unit (Keithley 237).

2.5. Microstructure examination

The either surface of samples that the electrical measurement has been finished was lapped and ground with SiC paper and polished with 0.3 μm-Al_2O_3 powder to a mirror-like surface. The polished samples were thermally etched at 1100–1150 °C for 10–30 min. The surface of samples was metallized with a thin coating of Au to reduce charging effects and to improve the resolution of the image. The surface microstructure was examined by a scanning electron microscope (SEM, Hitachi S2400, Japan). The average grain size (d) was determined by the lineal intercept method, given by $d = 1.56L/MN$ [13], where L is the random line length on the micrograph, M is the magnification of the micrograph, and N is the number of the grain boundaries intercepted by lines. The compositional analysis of the selected areas was determined by an attached energy dispersion X-ray analysis (EDAX) system. The crystalline phases were identified by an X-ray diffractometry (XRD, Rigaku D/max 2100, Japan) using a Cu K_α radiation. The density of ZPCE ceramics was measured by the Archimedes method.

3. Results and discussion

Fig. 1 shows the density of ZPCE ceramics with increasing Er_2O_3 additive content at 1300 °C and 1350 °C. The ceramics sintered at 1300 °C exhibited relatively low density in the range of 4.87–5.08 g/cm^3, that is, 84–88% of the theoretical density (TD) of pure ZnO (5.78 g/cm^3). The density of ceramics sintered at 1350 °C increased as Er_2O_3 additive content is increased up to 0.5 mol%. However, the density of ceramics decreased as Er_2O_3 additive content is further

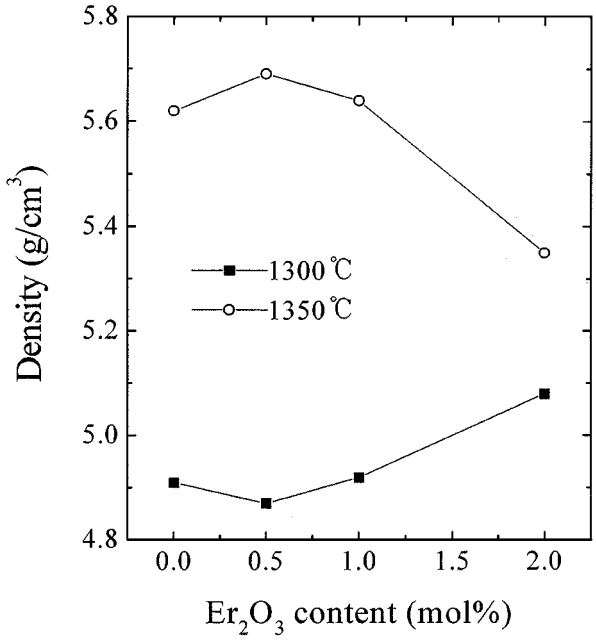

Figure 1 The density of ZPCE ceramics with Er_2O_3 additive content sintered at 1300 °C and 1350 °C.

increased. A maximun density of 5.69 g/cm^3 that corresponds to 98% of TD was obtained from ceramics doped with 0.5 mol% Er_2O_3. The ceramics sintered at 1350 °C exhibited relatively high density in the range of 5.35–5.69 g/cm^3, that is, 93–98% of TD. It can be seen that the density variation of ceramics sintered at 1350 °C shows an opposite relationship to that at 1300 °C. Therefore, it is clear that the density of ceramics was strongly influenced by Er_2O_3 additive content and sintering temperature. And as shown in SEM micrographs in Fig. 2, the ceramics sintered at 1300 °C were found to comprise many pores, compared with the ceramics sintered at 1350 °C. The density greatly affects the stability, which will be discussed later. The average grain size was 7.44, 6.96, 6.51, 5.62 μm at 1300 °C and 18.36, 15.69, 9.61, 9.11 μm at 1350 °C with increasing Er_2O_3 additive content. The tendency of decrease in the average grain size directly affects the varistor voltage in the electrical properties.

The XRD pattern shown in Fig. 3 revealed that the ZPCE ceramics have a secondary phase such as Er- and Pr-rich phase, in addition to the hexagonal ZnO. There were no any phases except for only two phases regardless of sintering temperatures. Er and Pr oxides were found to coexist at the grain boundaries and the nodal points as if they were a single phase, as shown in the EDAX analysis in Fig. 4. No Er peak into ZnO grains was found within EDAX detection limit. It is believed that this is attributed to the segregation of Er toward grain boundaries due to the difference of ionic radius. It was observed, by SEM that, as Er_2O_3 additive content increases, the intergranular phase such as Er- and Pr-rich phase was gradually more distributed at the grain boundaries and the nodal points, particularly. On the other hand, it was found, by XRD that Pr-rich phase are Pr_6O_{11} at 1300 °C and Pr_2O_3 at 1350 °C. Alles *et al.* reported that when Co/Pr mole ratio is above 4/1, the liquid-phase sintering have occurred at 1350 °C [6]. In the light to these facts, because Co/Pr mole ratio in this study is 2/1, it is believed that the ZPCE ceramics became the solid-phase sintering at 1300 °C and liquid-phase sintering at 1350 °C. According to the EDAX analysis, Er peak in intergranular layer was slightly higher than Pr peak at 1300 °C, whereas Pr peak was far higher rather than Er peak at 1350 °C. It can be seen that Er was somewhat volatile due to liquid-phase sintering at 1350 °C.

Fig. 5 shows the current density-electric field (J-E) characteristics of ZPCE varistors. The Er_2O_3 additive content dependence of the J-E characteristics for the varistors sintered at 1350 °C was larger than that of 1300 °C. In other words, the characteristic curves were collected in one place at 1300 °C, whereas they were scattered at 1350 °C. More detailed I-V characteristic parameters, including the varistor voltage ($V_{1\,mA}$), varistor voltage per grain boundaries (V_{gb}), nonlinear exponent (α), and leakage current (I_ℓ) are summarized in Table I. As can be seen in the table, the varistor voltage was increased in the range of 337.4–575.4 V/mm at 1300 °C and 8.9–324.7 V/mm at 1350 °C with increasing Er_2O_3 additive content. This is attributed to the decrease of average grain size with increasing Er_2O_3 additive content. It is believed that the large difference of varistor voltage with the increment of sintering temperature is attributed to the average grain size, that is, the larger the grain size, the lower the varistor voltage. The varistor voltage per grain boundaries (V_{gb}) is defined by $V_{gb} = (d/D)\ V_{1\,mA}$, where d is the average grain size and D is thickness of sample. It was increased in the range of 2.5–3.2 V/gb at 1300 °C and 0.2–3.0 V/gb at 1350 °C with increasing Er_2O_3 additive content. For ZPCE varistors sintered at 1300 °C, the nonlinear exponent was 29.7 in the case without Er_2O_3, whereas was

TABLE I The current-voltage (I-V) and capacitance-voltage (C-V) characteristic parameters of ZPCE varistors with Er_2O_3 additive content sintered at 1300 °C and 1350 °C

Sintering Temp.	Er_2O_3 content (mol%)	$V_{1\,mA}$ (V/mm)	V_{gb} (V/gb)	α	I_ℓ (μA)	N_d ($\times 10^{18}$ cm^{-3})	N_t ($\times 10^{12}$ cm^{-2})	ϕ_b (eV)	t (nm)
1300 °C	0.0	337.4	2.5	29.7	28.2	1.67	3.64	0.85	21.85
	0.5	416.3	2.9	52.8	9.8	1.21	2.90	0.74	23.93
	1.0	457.7	3.0	45.0	15.8	1.24	4.63	1.84	37.23
	2.0	575.4	3.2	44.9	19.2	0.65	2.67	1.17	41.31
1350 °C	0.0	8.9	0.2	2.1	133.8	14.63	6.30	0.29	4.30
	0.5	105.8	1.7	34.8	7.4	4.11	5.11	0.68	12.43
	1.0	231.3	2.2	36.8	5.9	2.81	4.85	0.89	17.29
	2.0	324.7	3.0	29.9	13.3	1.69	4.20	1.11	24.75

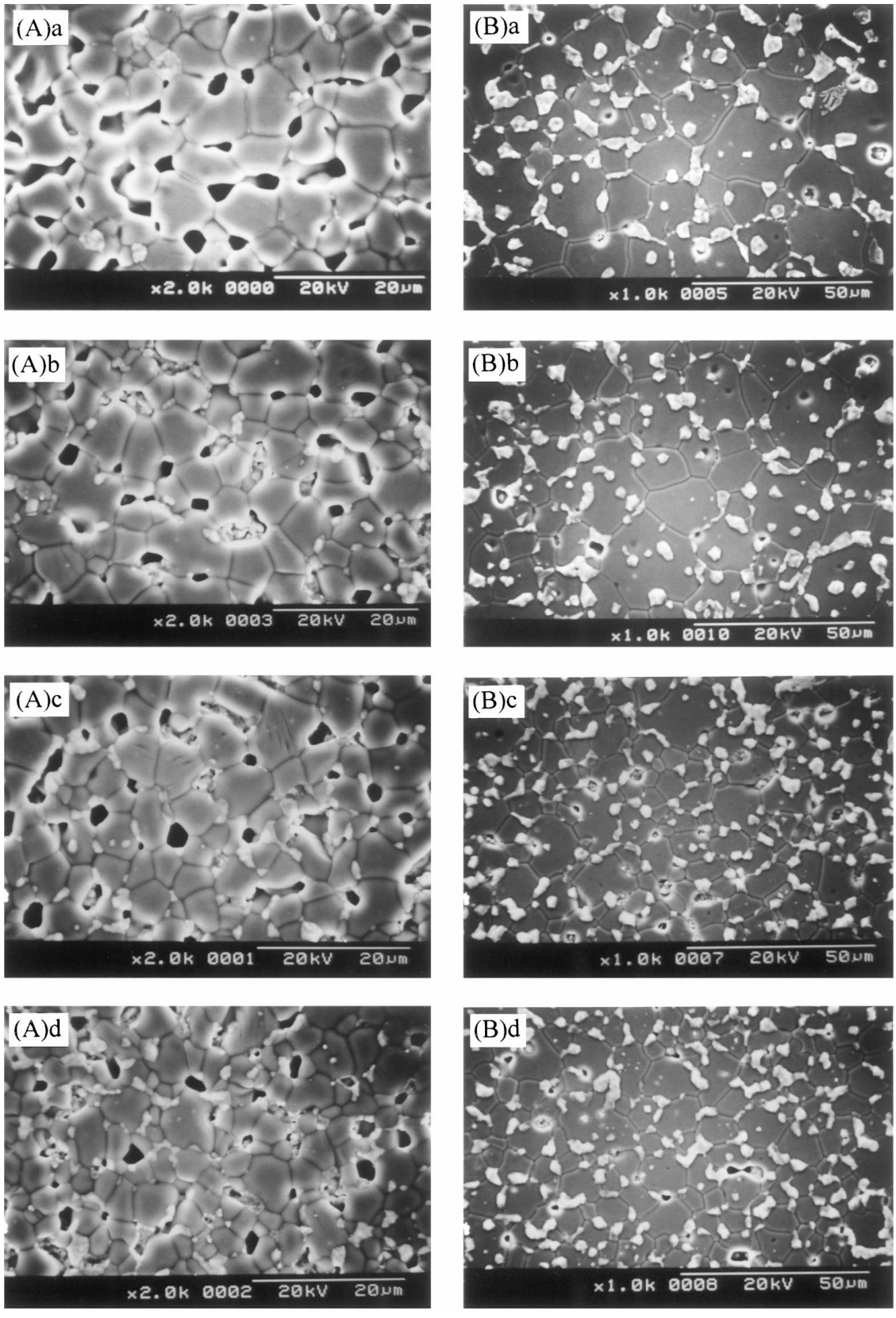

Figure 2 SEM micrographs of ZPCE ceramics with Er_2O_3 additive content sintered at (A) 1300 °C and (B) 1350 °C. a: 0.0 mol%, b: 0.5 mol%, c: 1.0 mol%, and d: 2.0 mol%.

largely increased in the range of 44.9–52.8 in the case with Er_2O_3. In particular, the varistors with 0.5 mol% Er_2O_3 exhibited the best nonlinear I-V characteristics, which are 52.8 in the nonlinear exponent and 9.8 μA in the leakage current. The addition of Er_2O_3 above 0.5 mol% rather deteriorated I-V characteristics. For ZPCE varistors sintered at 1350 °C, the varistors without Er_2O_3 exhibited very poor nonlinear properties indicating 2 in the nonlinear exponent and 133.8 μA in the leakage current, whereas the varistors with Er_2O_3 exhibited relatively good nonlinear properties, which the nonlinear exponent is in the range of 29.9–36.8. In

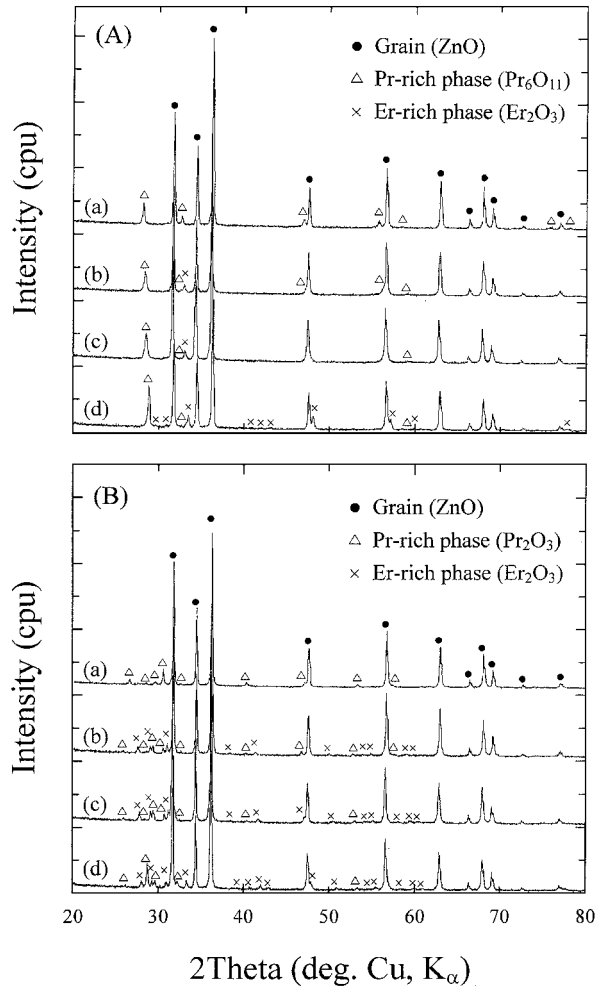

Figure 3 XRD patterns of ZPCE ceramics with Er_2O_3 additive content sintered at (A) 1300 °C and (B) 1350 °C. (a) 0.0 mol%, (b) 0.5 mol%, (c) 1.0 mol%, and (d) 2.0 mol%.

particular, the varistors with 1.0 mol% Er_2O_3 exhibited the best nonlinear I-V characteristics, which are 36.8 in the nonlinear exponent and 5.9 μA in the leakage current. As a result, the addition Er_2O_3 to the ternary system ZnO-Pr_6O_{11}-CoO greatly improved I-V characteristics in terms of without and with Er_2O_3 addition. And the nonlinear exponent was far higher at 1300 °C than that of 1350 °C, whereas the leakage current was low at 1350 °C rather than that of 1300 °C.

Fig. 6 shows the C-V characteristics of ZPCE varistors. More detailed C-V characteristic parameters, including the donor concentration (N_d), density of interface states (N_t), barrier height (ϕ_b), and depletion layer width (t) are summarized in Table I. The donor concentration was decreased in the range of 1.67×10^{18}–0.65×10^{18} cm^{-3} at 1300 °C and 14.63×10^{18}–1.69×10^{18} cm^{-3} at 1350 °C with increasing Er_2O_3 additive content. This means Er_2O_3 acts as an acceptor. Although Er^{+3} ions have a larger radius (0.088 nm) than Zn^{+2} ions (0.074 nm), limited substitution within the ZnO grains is possible. Er substitutes for Zn and creates lattice defect in ZnO grains. The chemical-defect reaction using Kroger-Vink notation can be written as $Er_2O_3 \xrightarrow{ZnO} 2Er_{Zn}^{\cdot} + V_{Zn}'' + 2O_o^{\times} + 1/2O_2$, where $Er_{Zn}^{\cdot}$ is a positively charged Er ion substituted for Zn lattice site, V_{Zn}'' is a negatively charged Zn vacancy, and $O_o^{\times}$ is a neutral oxygen of oxygen lattice site. The oxygen generated in reaction above affects the donor concentration. In other words, N_d is related to the partial pressure of oxygen (Po_2), namely, $N_d \propto Po_2^{-1/4}$ or $Po_2^{-1/6}$. It is, therefore, believed that the decrease of donor concentration with Er_2O_3 additive content is attributed to the increase of partial pressure of oxygen. The density of interface states was not, especially, related to Er_2O_3 additive content at 1300 °C, whereas it was decreased in the range of 6.30×10^{12}–4.20×10^{12} cm^{-2} at 1350 °C. The barrier height exhibit the same tendency as the density of interface states at 1300 °C, whereas it was increased in the range of 0.29–1.11 eV at 1350 °C. By the way, the barrier height is directly connected with the donor concentration and density of interface states. In other words, the barrier height is estimated by the variation rate in the density of

TABLE II Variation of I-V characteristic parameters in of ZPCE varistors with Er_2O_3 additive content during various d.c. stress sintered at 1350 °C

Er_2O_3 content (mol%)	Stress conditions	$V_{1\,mA}$ (V/mm)	$\%\Delta V_{1\,mA}$	α	$\%\Delta\alpha$	I_ℓ (μ A)	$\%\Delta I_\ell$
0.0	Before	8.9	0	2.1	0	133.8	0
	First	7.9	−11.2	2.0	−4.8	135.6	1.3
	Second	6.5	−27.0	1.9	−9.5	139.1	4.0
	Third	5.8	−34.8	1.8	−14.3	140.2	4.8
	Fourth	5.4	−39.3	1.8	−14.3	140.6	5.1
0.5	Before	105.8	0	34.8	0	7.4	0
	First	105.9	0.1	35.6	2.3	5.3	−28.4
	Second	105.4	−0.4	34.6	−0.6	6.7	−9.5
	Third	104.9	−0.9	33.8	−2.9	7.6	2.7
	Fourth	105.7	−0.1	29.1	−16.4	18.8	154.1
1.0	Before	231.3	0	36.8	0	5.9	0
	First	231.8	0.2	37.7	2.4	5.4	−8.5
	Second	229.8	−0.6	34.6	−6.0	7.8	32.2
	Third	228.4	−1.3	33.2	−9.8	7.7	30.5
	Fourth			Thermal runaway			
2.0	Before	324.7	0	29.9	0	13.3	0
	First	321.9	−0.9	27.8	−7.0	14.8	11.3
	Second			Thermal runaway			

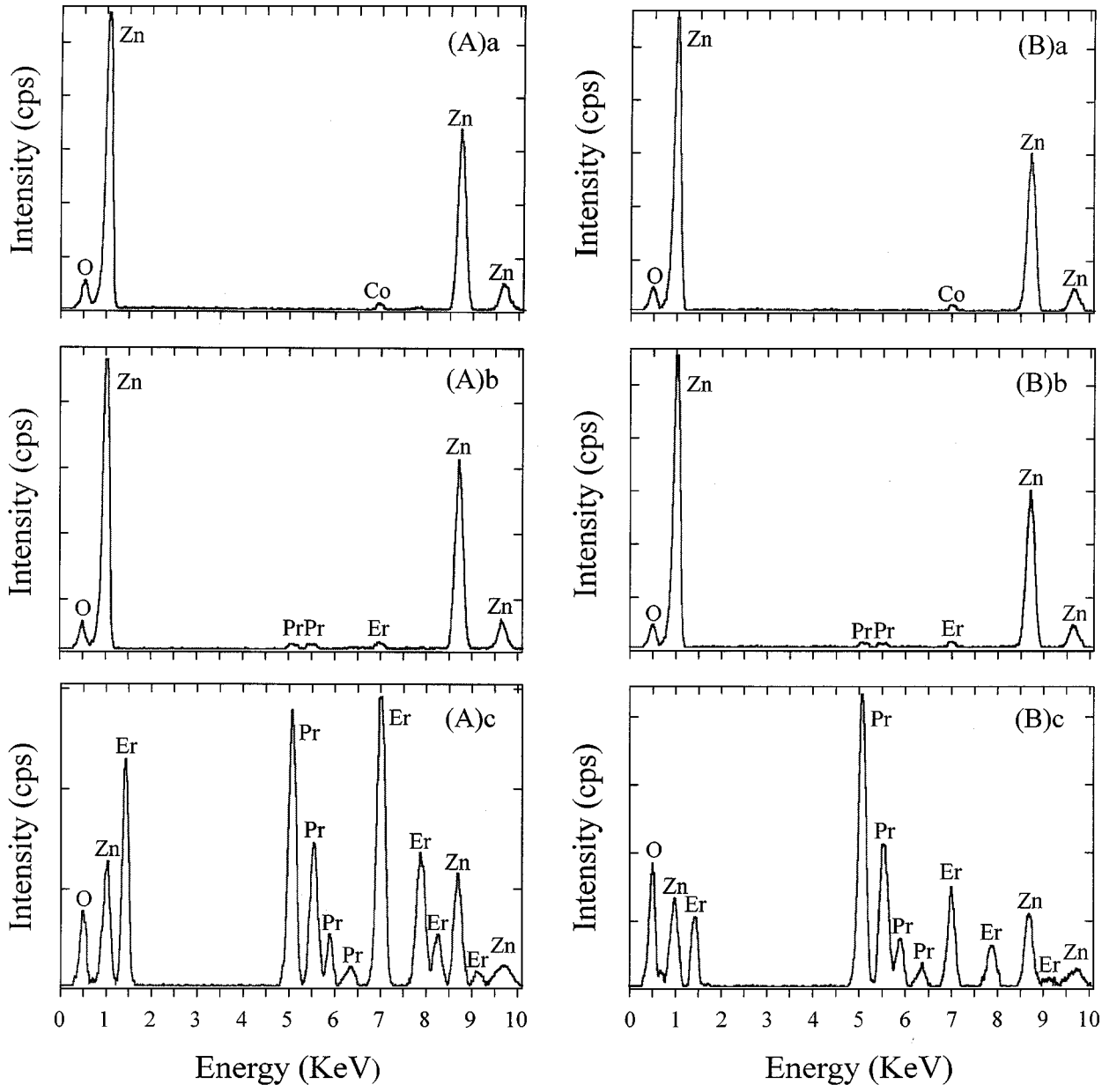

Figure 4 EDAX analysis of ZPCE ceramics with Er_2O_3 additive content sintered at (A) 1300 °C and (B) 1350 °C. a: ZnO grain, b: grain boundary, and c: nodal point.

interface states and donor concentration. Generally, the barrier height is increased with increasing density of interface states and decreasing donor concentration. If the variation rate of donor concentration is much larger than that of density of interface states with an additive content, the barrier height is much more strongly affected the donor concentration than the density of interface states. According to this reason, it can be understood that the barrier height is increased or decreased with increasing Er_2O_3 additive content. The increase of depletion layer width for both sintering temperatures, with increasing Er_2O_3 additive content, is attributed to the decrease of donor concentration.

Fig. 7 shows the leakage current during the first d.c. stress of ZPCE varistors sintered at 1300 °C. The varistors, even under relatively weak stress, exhibited the thermal runaway within short time in order of high leakage current indicated in Table I. After the stress, eventually, these varistors were completely degraded. It is believed that this result is attributed to the high leakage current, whereas more attributed to the low density of ceramics. In other words, the varistors are fast degraded because the low density decreases the number of parallel conduction path and eventually leads to the concentration of current.

Fig. 8 shows the leakage current during various stresses of ZPCE varistors sintered at 1350 °C. Above all, it can be surely seen that ZPCE varistors sintered at 1350 °C are far more stable than that at1300 °C. It is believed that this is attributed to the much higher density and the lower leakage current. The varistors without Er_2O_3 exhibited relatively weak positive creep phenomena of the leakage current with various stresses. Moreover, it showed rather negative creep phenomena during the fourth stress. Although the leakage current is very high, to not appear the thermal run away is likely to due to ohmic-like properties, which are extremely low

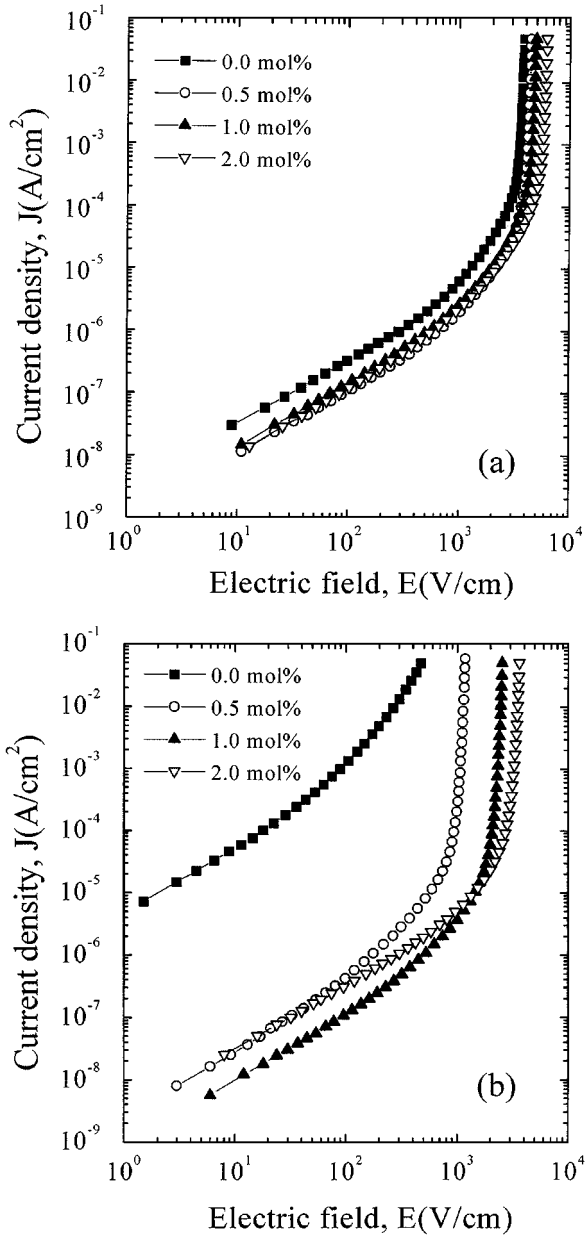

Figure 5 The current density-electric field (J-E) characteristics of ZPCE varistors with Er_2O_3 additive content sintered at (a) 1300 °C and (b) 1350 °C.

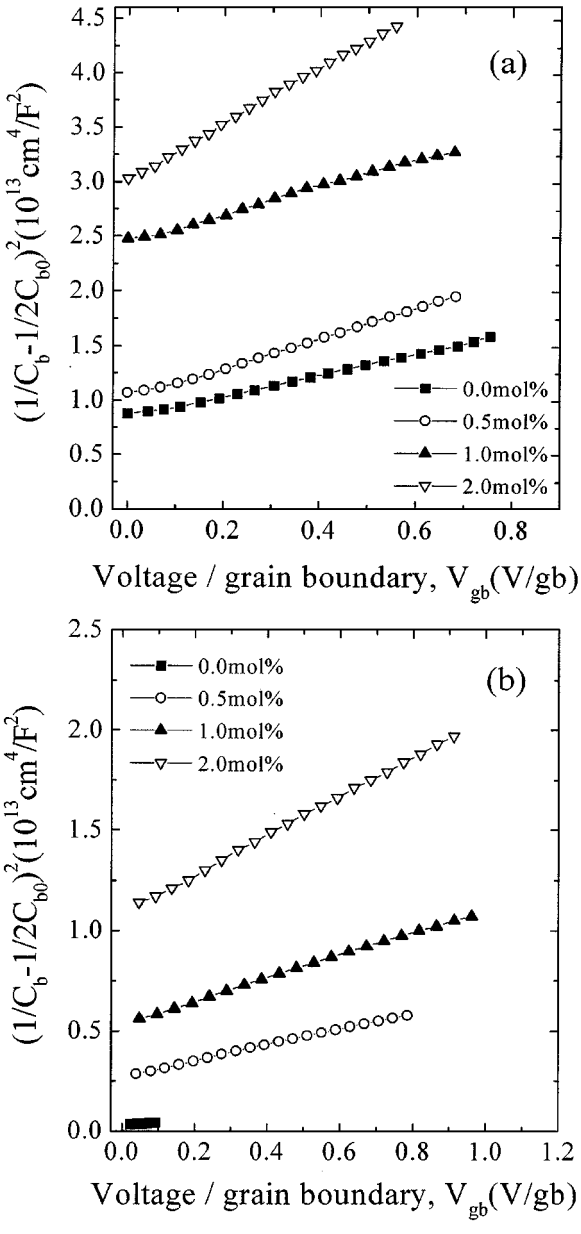

Figure 6 The capacitance-voltage (C-V) characteristics of ZPCE varistors with Er_2O_3 additive content sintered at (a) 1300 °C and (b) 1350 °C.

nonlinearity. The varistors with 1.0 and 2.0 mol% Er_2O_3 exhibited the thermal runaway at the fourth and second stress, respectively. Meanwhile, the varistors with 0.5 mol% Er_2O_3, even under the fourth stress, exhibited the positive creep of leakage current instead of the thermal run away. Therefore, the varistors with 0.5 mol% Er_2O_3 is believed to show the best stability.

The detailed variation of I-V characteristic parameters after various stresses is summarized in Table II. For the varistors without Er_2O_3, the variation rate of the varistor voltage ($\%\Delta V_{1\,mA}$) marked above 10%. The varistors with 1.0 mol% Er_2O_3 exhibited very good stability having $\%\Delta V_{1\,mA} < 2\%$ after the third stress, but thermal runaway thereafter. The varistors with 2.0 mol% Er_2O_3 were relatively stable after the first stress, but thermal runaway thereafter. While, the varistors with 0.5 mol% Er_2O_3 exhibited very weak positive creep of leakage current, close to

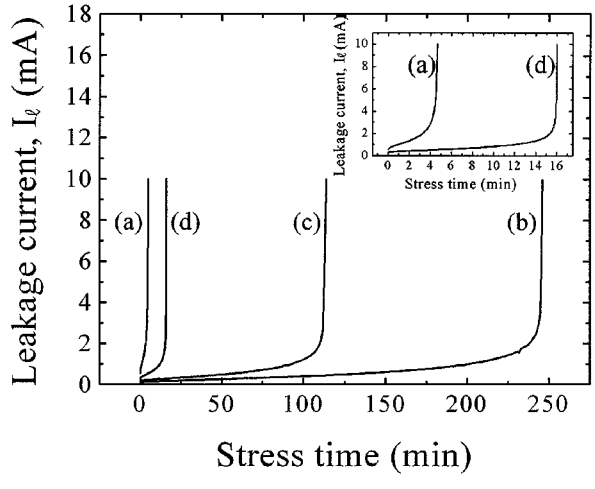

Figure 7 Leakage current of ZPCE varistors with Er_2O_3 additive content during the first d.c. stress sintered at 1300 °C. (a) 0.0 mol%, (b) 0.5 mol%, (c) 1.0 mol%, and (d) 2.0 mol%.

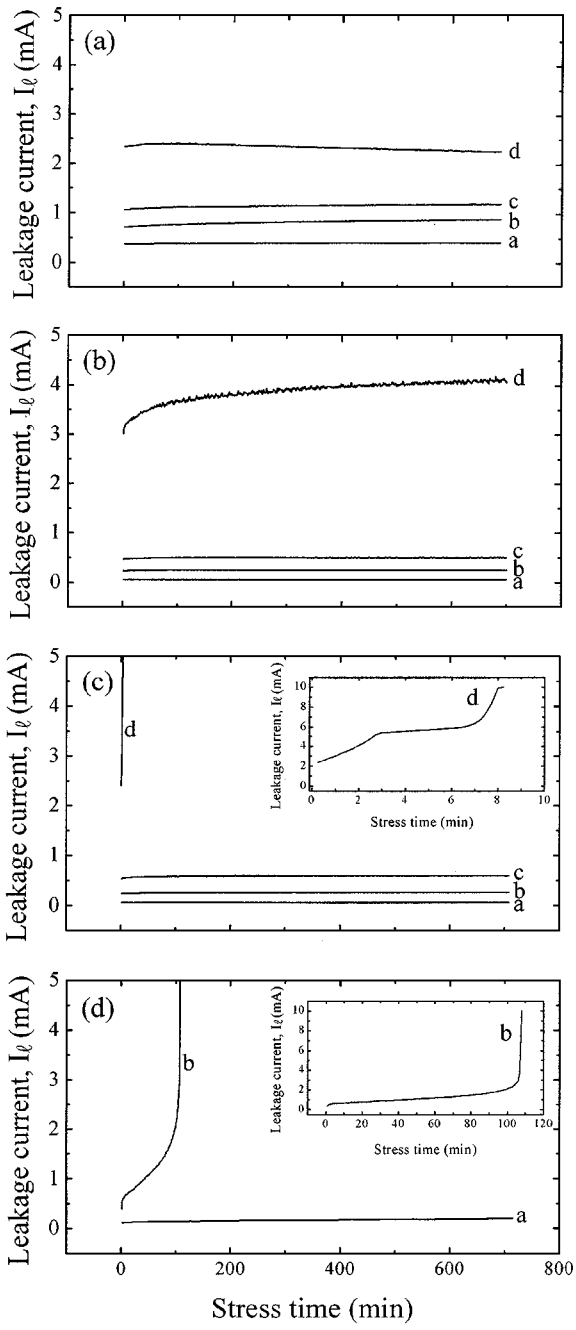

Figure 8 Leakage current of ZPCE varistors with Er_2O_3 additive content during various d.c. stresses sintered at 1350 °C, (a) 0.0 mol%, (b) 0.5 mol%, (c) 1.0 mol%, and (d) 2.0 mol%. a: the first stress, b: the second stress, c: the third stress, and d: the fourth stress.

nearly constant current during the third stress. Consequently, they marked $\%\Delta V_{1\,mA} < 1\%$, $\%\Delta\alpha < 3\%$, and $\%\Delta I_\ell < 3\%$ after the third stress. Moreover, even by the fourth stress, unexpectedly, it is the fact that they revealed the nearly same $V_{1\,mA}$ as that before the stress. In the light of general facts that the allowed specifications of $\%\Delta V_{1\,mA}$ under d.c. stress in the commercial varistors are less than 10%, it can be seen that the varistors with 0.5 mol% Er_2O_3 possess very excellent stability. For the ZPCE varistors sintered at 1350 °C, the nonlinearity was somewhat bad than that at 1300 °C, but the stability was good rather than that 1300 °C. In the light of these facts, to improve the stability, the leakage current should be, of course, low, but the density should be high. Of the varistors sintered at 1350 °C, comparing 0.5 mol% Er_2O_3 with 1.0 mol% Er_2O_3-added varistors, the former has slightly higher ceramic density, the latter has slightly lower leakage current. If so, which of the varistors is the stability better? The answer for this query is that the densified microstructure is more important than any other things.

The degradation of ZnO varistors is associated with the lowering of the potential barrier at the grain boundaries, which is related to the annihilation of interface defect states when stressed continuously by an electric field [14]. The positively charged zinc interstitial (Zn_i) formed to the depletion layer migrates toward the negatively charged grain boundary interface during stress period and it recombines with zinc vacancy (V_{Zn}) positioned in there. As a result, the recombination of these species leads to the degradation of ZnO varistors. Based on these facts, it is guessed that the reason why the varistors with Er_2O_3 of 0.5 mol% exhibit very excellent stability is because the added-Er_2O_3 spatially restricts the migration of zinc interstitial (Zn_i) within depletion layer or stabilizes the interface states.

4. Conclusions

The microstructure, electrical properties, and stability of Pr_6O_{11}-based ZnO varistors, which are composed of ZnO-Pr_6O_{11}-CoO-Er_2O_3 systems, were investigated with Er_2O_3 additive content at 1300 °C and 1350 °C. The ceramics sintered at 1350 °C was far more densified than that of 1300 °C and highly densified ceramics were obtained by doping with 0.5 mol% Er_2O_3. Most of the added-Er_2O_3 were segregated at nodal points and grain boundaries, and found to form Er-rich phase together with Pr-rich phase. In addition, the integranular layer was consisted of the Er- and Pr-rich phase. The addition Er_2O_3 to the ternary system ZnO-Pr_6O_{11}-CoO greatly improved I-V characteristics in terms of without and with Er_2O_3 addition, and the nonlinear exponent is far higher at 1300 °C than that of 1350 °C, whereas the leakage current is low at 1350 °C rather than that of 1300 °C. All the varistors sintered at 1300 °C, even under relatively weak stress, exhibited the thermal runaway within short time in order of high leakage current. On the contrary, the stability of varistors sintered at 1350 °C were far higher than that at1300 °C. In particular, the varistors with 0.5 mol% Er_2O_3 showed not only relatively good nonlinear I-V characteristics, but also excellent stability, which the variation rates of varistor voltage, nonlinear exponent, and leakage current are below 1%, 3%, and 3%, respectively, even under more severe stress such as (0.80 $V_{1\,mA}$/90 °C/12 h) + (0.85 $V_{1\,mA}$/115 °C/12 h) + (0.90 $V_{1\,mA}$/120 °C/12 h). Consequently, it was estimated that the 98.0 mol% ZnO-0.5 mol% pr_6O_{11}-1.0 mol% CoO-0.5 mol% Er_2O_3 ceramics will be used as basic composition to develop the advanced Pr_6O_{11}-based ZnO varistors having the high performance and stability in the future.

Acknowledgement

This work has been supported in part by Electrical Engineering & Science Research Institute, Grant, 99-016,

which is funded under support of Korea Electric Power Corporation.

References

1. L. M. LEVINSON and H. R. PILIPP, *Am. Ceram. Soc. Bull.* **65** (1986) 639.
2. T. K. GUPTA, *J. Amer. Ceram. Soc.* **73** (1990) 1817.
3. S. Y. CHUN, N. WAKIYA, K. SHNOZAKI and N. MIZUTANI, *Jpn. J. Ceram. Soc.* **104** (1996) 1056.
4. Y. S. LEE and T. Y. TSENG, *J. Amer. Ceram. Soc.* **75** (1992) 1636.
5. A. B. ALLES and V. L. BURDICK, *J. Appl. Phys.* **70** (1991) 6883.
6. A. B. ALLES, R. PUSKAS, G. CALLAHAN and V. L. BURDICK, *J. Amer. Ceram. Soc.* **76** (1993) 2098.
7. Y.-S. LEE, K.-S. LIAO and T.-Y. TSENG, *ibid.* **79** (1996) 2379.
8. C.-W. NAHM and C.-H. PARK, *J. Mater. Sci.* **35** (2000) 3037.
9. C.-W. NAHM, C.-H. PARK and H.-S. YOON, *J. Mater. Sci. Lett.* **19** (2000) 271.
10. *Idem., ibid.* **19** (2000) 725.
11. M. MUKAE, K. TSUDA and I. NAGASAWA, *J. Appl. Phys.* **50** (1979) 4475.
12. L. HOZER, "Semiconductor Ceramics: Grain Boundary Effects" (Ellis Horwood, 1994) p. 22.
13. J. C. WURST and J. A. NELSON, *J. Amer. Ceram. Soc.* **97-12** (1972) 109.
14. T. K. GUPTA and W. G. CARLSON, *J. Mater. Sci.* **20** (1985) 3487.

Received 17 March
and accepted 19 October 2000